

Residual Bearing Capabilities of Fire-Exposed Reinforced Concrete Beams

J. H. Hsu^{1,2,*} and C. S. Lin²

¹*Department of Civil Engineering, Ching Yun University,
Jung-Li 320, Taiwan*

²*Department of Mechanical Engineering, Yuan Ze University,
Jung-Li 320, Taiwan*

Abstract: This work combines thermal and structural analyses to assessing the residual bearing capabilities, flexural and shear capacities of reinforced concrete beams after fire exposure. The thermal analysis uses the finite difference method to model the temperature distribution of a reinforced concrete beam maintained at high temperature. The structural analysis, using the lumped method, is utilized to calculate the residual bearing capabilities, flexural and shear capacities of reinforced concrete beams after fire exposure. The results of the thermal analysis are compared to the experimental results in the literature, and the analytically derived structural results are also compared with full-scale reinforced concrete beams in previous fire exposure experiments. The comparison results indicated that the calculation procedure in this study assessed the residual bearing capabilities of reinforced concrete beams exposed to fire with sufficient accuracy. As no two fires are the same, this novel scheme for predicting residual bearing capabilities of fire-exposed reinforced concrete beams is very promising in that it eliminates the extensive testing otherwise required when determining fire ratings for structural assemblies.

Keywords: Residual, bearing capabilities, fire-exposed, RC beams

1. Introduction

Fire is a destructive force that causes thousands of deaths and billions in property loss annually. People around the world expect that their homes and workplaces will be safe from the ravages of an unwanted fire. Unfortunately, fires can occur in almost any kind of building, often when least expected. More than 90% of the buildings in Taiwan are reinforced concrete (RC) structures. Moreover, Taiwan is situated in a seismic region. Whether RC structures are sufficiently strong to withstand an earthquake following fire damage is extremely important to human life

and property. The fire safety of RC structures largely depends on their fire resistance, which in turn depends on the combustibility and fire resistance of their main structural elements, i.e., beams and columns. As structural elements, beams are subject to flexural and shearing loads. The residual bending moment and shear force of fire-damaged concrete beams are important factors in determining the safety of the structure.

The properties of the constituent materials of RC beams, concrete and steel, in terms of strength and stiffness are progressively reduced by the increasing temperature. Modulus of elasticity and shear modulus decrease with

* Corresponding author; e-mail: rhhsu@cyu.edu.tw

Accepted for Publication: August 29, 2006

the increase of temperature [1]. Numerous studies have investigated the effects of fire on concrete [2, 3, 4], whereas other have examined the effects of fire on steel [2, 4–6].

Analyzing the bearing capability of RC beams after sustaining fire requires the knowledge of temperature distribution in the cross sections. This is determined by the thermal properties of the material, such as the heat capacity and thermal conductivity. A simple thermal model, which is generally to all beams with a rectangular cross section, has been assessed in a separate series of studies which were also reported in a previous paper [7]. The modeling results achieved reasonable agreement with isothermal contours obtained by Lin [8], who analyzed the temperature distribution of pure concrete according to the time-temperature curve of standard fire.

The analytical stage in the modeling process is to increment the time of the model such that the temperature experienced by the beam is increased. The increase in the ambient temperature changes the temperature distribution inside of beam's cross-sections. After sustaining high temperature, the mechanical properties of reinforced steel and concrete vary according to the fire-induced temperature. It makes the stress distribution in such beam structures a nontrivial problem. The structural analysis in this model follows American Concrete Institute (ACI) building code, which considers the influence of temperature on reinforced steel and concrete using a lumped system method to determine flexural and shear capacities. Modeling results for flexural capacities have been compared to the calculated results using the ACI code at room temperature and also compared with full-scale RC beam fire exposure experiments [9]. The analytically derived shear capacities have also been compared with experimental data [10]. The consistency between modeling and experimental results has confirmed the accuracy of this model.

2. Flexural capacity of RC beams exposed fire

The flexural capacity of a beam is the ultimate bending moment that can be sustained by the beam in flexure before failure occurs. The ACI code [11] provides a general expression for the balanced state that links the tensile strength of reinforced steels, compressive strength of concrete, their respective moduli and the reinforcement ratio ρ . The balanced steel ratio, ρ_b , is determined by identifying the reinforcement ratio of a balanced condition where failure would occur simultaneously in the concrete and reinforced steels. In order to ensure yielding of steel before crushing of concrete, the code provisions are intended to ensure a ductile mode of failure by limiting the amount of tension reinforcement ratio, ρ_{max} , to 75% of ρ_b . The flexural failure in the case of RC beams with a very small amount of tensile reinforcement can be sudden. To prevent such a failure, a minimum amount of tensile reinforcement ratio, ρ_{min} is required.

Equilibrium between the compressive and tensile forces acting on the beam cross section at nominal strength should be satisfied when the beam computed by the strength design method of the code. In rectangular sections of beams with tension reinforcement only, the equilibrium conditions are as follows:

Force equilibrium:

$$C = T \quad (1)$$

$$0.85f'_c ab = A_s f_y = \rho b d f_y$$

$$a = \frac{A_s f_y}{0.85 f'_c b} = \frac{\rho d f_y}{0.85 f'_c}$$

Moment equilibrium:

$$\begin{aligned} M_n &= (C \text{ or } T) \left[d - \frac{a}{2} \right] \\ &= \rho b d f_y \left[d - 0.59 \rho d \frac{f_y}{f'_c} \right] \end{aligned} \quad (2)$$

The stress-related strain includes the elastic and plastic components of strain resulting from applied stress. From the stress-strain relationships for concrete at elevated temperatures, the stress-strain relationship of concrete is a function of temperature [12]. The residual compressive stress and elastic modulus of concrete after exposure to high temperature decline as temperature increases. The residual compressive stress of concrete under sustained elevated temperature can thus be retrieved from a given temperature and strain.

This work considers the fire-related factors that affect reinforcement bars and concrete materials using the lumped system method, and determines the residual ultimate bending moments of RC beams after fire damage.

The lumped system concept is taken from thermal conduction models. When heat is transferred through a medium, the temperature varies with time and position. Under particular conditions, temperature varies only linearly with time; such a system is called a Lumped System [13]. The concept underlying the original lumped system is extended such that following separation, material temperature and mechanical characteristics do not vary with position. The temperature and mechanical properties of the unit are assumed to be everywhere the same as those at the center of the unit. In this work, the cross section of an RC beam is divided into $M \times N$ segments for analysis. Each segment is considered to have a uniform (but different) temperature and iso-properties, according to the lumped system concept. A computer program was developed to calculate the residual bending moment of reinforced concrete beams after exposure. Figure 1 presents the calculation flowchart of the program.

The strain at extreme concrete compression fiber is first assumed as ε_{cp} . A distance from the extreme compression fiber to the neutral axis, c , is then defined. Combining the temperature distribution of the cross-section calculated from the thermal model and the strain,

a residual compressive stress matrix can be obtained from the stress-strain relationships in [12].

The tensile strength of the cross section of RC beams can be derived by

$$T_{en} = A_s \cdot f_{yr} \quad (3)$$

The reduction in yielding strength of steel is defined by a number of points. Eurocode 3 [14] gives an expression of approximate curve for the reduction in yielding strength of steel.

$$k_{y,T} = [0.9674(1 + \exp[(T - 482)/39.19])]^{-1/3.833} \quad (4)$$

Where $k_{y,T}$ is the ratio of f_{yr} (the yield strength at elevated temperature) to f_y (the yield strength at 20° C).

The compressive strength of the cross-section of RC beams can be calculated by summing all the compressive strengths on the compressive side of lumped units.

$$C = \sum_{i=1}^M \sum_{j=1}^{c/\Delta y} f_{c,ij}^T \cdot \Delta x \cdot \Delta y \quad (5)$$

If the sectional stress of the cross section is in static equilibrium, Eqs. (3) and (5) should be equal. If not, the assumed c value is suspected to be too small to satisfy the equilibrium. In this case, the value of c is increased and the calculation is repeated. If the equilibrium remains unsatisfactory with the adjusted c value, we assume that ε_{cp} is too small and ε_{cp} is increased. This process continues until Eqs. (3) and (5) are equal.

When the beam cross section is in static equilibrium, the residual ultimate moment of the beam M_u can be calculated as

$$M_u = A_s \cdot f_{yr} \cdot \left(d - \frac{\sum_{i=1}^M \sum_{j=1}^{c/\Delta y} f_{c,ij}^T \cdot \Delta x \cdot \Delta y \cdot j \cdot \Delta y}{\sum_{i=1}^M \sum_{j=1}^{c/\Delta y} f_{c,ij}^T \cdot \Delta x \cdot \Delta y} \right) \quad (6)$$

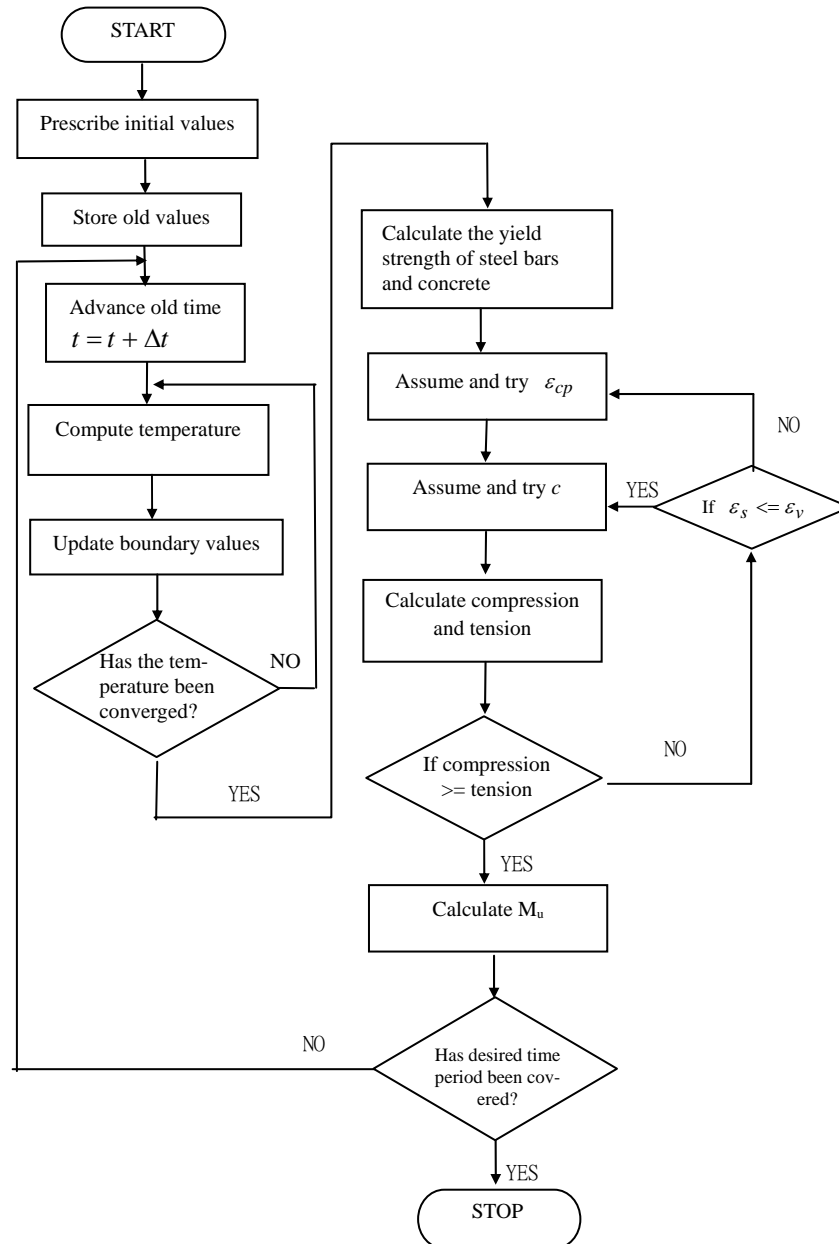


Figure 1. Flowchart for modeling the residual flexural capacity of RC beam exposed to fire

3. Shear capacity of RC beams exposed to fire

According to the ACI code [11], the nominal shear strength of an RC beam can be determined as

$$V_n = V_c + V_s \quad (7)$$

For normal beams ($l_n/d > 5$) subject to shear and flexure only, (The formulas are trans-

formed to SI units)

$$V_c = (0.50\sqrt{f'_c} + 176\rho\frac{V_u d}{M_u})bd \leq 0.93\sqrt{f'_c}bd \quad (8)$$

$$V_s = A_v f_y d / s \quad (9)$$

For deep beams ($l_n/d < 5$), (The formulas are transformed to SI units)

$$V_c = (3.5 - 2.5\frac{M_u}{V_u d})(0.50\sqrt{f'_c} + 176\rho\frac{V_u d}{M_u})bd \leq 1.59\sqrt{f'_c}bd \quad (10)$$

$$V_s = \frac{A_v f_y d}{s} \left(\frac{1+L_n/d}{12} \right) + \frac{A_{vh} f_y d}{s_h} \left(\frac{11-L_n/d}{12} \right) \quad (11)$$

Based on ACI code assumptions [11] and the effects of temperature, the cross section is divided into $M \times N$ segments. Each segment can exhibit a uniform temperature and iso-properties. The shear strength of the RC beam cross section can be determined by summing the shear strengths of all of the lumped units. A computer program sums the residual strengths for all lumped units, as in Eqs. (12) – (17).

$$V_m = V_{rc} + V_{rs} \quad (12)$$

For normal beams, ($l_n/d > 5$)

$$\begin{aligned} V_{rc} &= \sum_{i=1}^n \sum_{j=1}^m V_{rc,ij} = V_{rc,11} + V_{rc,12} + \dots + V_{rc,21} \\ &+ V_{rc,22} + \dots + V_{rc,n1} + V_{rc,n2} + \dots + V_{rc,nm} \\ &= \sum_{i=1}^n \sum_{j=1}^m (0.50 \sqrt{f'_{cr,ij}} + 176 \rho \frac{V_u d}{M_u}) A_{ij} \leq \sum_{i=1}^n 0.93 \sqrt{f'_{cr,ij}} A_{ij}, \text{ and } \frac{V_u d}{M_u} \leq 1 \end{aligned} \quad (13)$$

$$V_{rs} = \frac{A_v f_{yr} d}{s} \quad (14)$$

where the subscript r is the residual value of the properties after the unit sustained high temperature, and f'_{cr} is the residual compressive strength of the concrete after heating. Experimental data obtained by Abrams [15] were used to derive a conservative formula for residual compressive strength of concrete exposed to high temperatures:

$$f'_{cr} = \begin{cases} (1 - 0.001T) f'_c & 0^\circ C \leq T \leq 500^\circ C \\ (1.375 - 0.00175T) f'_c & 500^\circ C \leq T \leq 700^\circ C \\ 0 & 700^\circ C \leq T \end{cases} \quad (15)$$

For deep beams, ($l_n/d < 5$)

$$\begin{aligned} V_{rc} &= \sum_{i=1}^n \sum_{j=1}^m V_{rc,ij} = V_{rc,11} + V_{rc,12} + \dots + V_{rc,21} \\ &+ V_{rc,22} + \dots + V_{rc,n1} + V_{rc,n2} + \dots + V_{rc,nm} \\ &= \sum_{i=1}^n \sum_{j=1}^m (3.5 - 2.5 \frac{M_u}{V_u d}) (0.50 \sqrt{f'_{r,ij}} + 176 \rho \frac{V_u d}{M_u}) A_{ij} \\ &\leq \sum_{i=1}^n \sum_{j=1}^m 1.59 \sqrt{f'_{cr,ij}} A_{ij}, \text{ and } (3.5 - 2.5 \frac{M_u}{V_u d}) \leq 2.5 \end{aligned} \quad (16)$$

$$V_{rs} = \frac{A_v f_{rs} d}{s} \left(\frac{1+L_n/d}{12} \right) + \frac{A_{vh} f_{rs} d}{s_h} \left(\frac{11-L_n/d}{12} \right) \quad (17)$$

4. Validation and discussion

At room temperature ($20^\circ C$), the ultimate bending moment M_u is calculated for beam cross sections of 20×40 cm, 30×45 cm and 30×60 cm with three steel ratios of ρ_{\min} , ρ_{\max} and $\frac{1}{2}(\rho_{\max} + \rho_{\min})$, given $f'_c = 210 \text{ kg/cm}^2$ and $f_y = 4200 \text{ kg/cm}^2$. Table 1 presents computational results for code and that obtained this study. Figure 2 presents a diagrammatic comparison of study and code results (Table 1). The code and modeling residual bending moments for typical dimensions are in good agreement, as determined by comparing the calculations for the non-fire situation with ACI code data.

Moetaz et al. [9] fabricated four reinforced beams 20 cm deep, 12 cm wide and 180 cm long. The beams were reinforced with 2ϕ 10mm grade 52 steel ($f_y = 3600 \text{ kg/cm}^2$) as the main reinforcement, 2ϕ 10 mm grade 37 steel ($f_y = 2600 \text{ kg/cm}^2$) as the secondary reinforcement, and $\Phi 8$ mm grade 37 stirrups with 8 cm spacing. The beams were installed in the fire test chamber 40 days after casting. During the fire test, the beams were not loaded and exposed to fire at $650^\circ C$ (Figure 3). The chamber was controlled so that the same average temperature-time curve was followed for all beams. Beams were exposed to fire for 30, 60 and 120 minutes and the control beam was not exposed to fire. After cooling to room temperature, the beams were tested to failure

by applying two increasing transverse loads (Figure 4). Table 2 presents the test and modeling results for beams (B, B₁, B₂ and B₃) that were exposed to fire for 0, 30, 60 and 120 minutes, respectively. Figure 5 shows the decreases in residual bending moment for experimental and modeling with duration of fire. Experimental and modeling results follow

similar trends and seem reasonable. Figure 6 diagrammatically compares the residual bending moment obtained between experimental and modeling results also. Agreement between experimental (code) and modeling results in Figures 2 and 6 shows that using the calculation procedure in this study is suitability.

Table 1. Ultimate bending moment from Code and modeling for various beam section and reinforcing ratios at room temperature

| Reinforcing ratio | 20cm×40cm | | 30cm×45cm | | 30cm×60cm | |
|--|-----------|----------|-----------|----------|-----------|----------|
| | Code | Modeling | Code | Modeling | Code | Modeling |
| ρ_{min} | 42.18 | 42.18 | 80.15 | 80.05 | 142.34 | 142.44 |
| $\frac{1}{2}(\rho_{max} + \rho_{min})$ | 127.43 | 128.51 | 241.91 | 243.97 | 429.97 | 434.39 |
| ρ_{max} | 193.75 | 196.79 | 367.97 | 373.66 | 654.03 | 664.92 |

kN-m

Table 2. Ultimate bending moment from experiment and modeling

| Properties | Beams | | | |
|--|-------|-------|-------|-------|
| | B | B1 | B2 | B3 |
| Fire exposure time(min.) | 0 | 30 | 60 | 120 |
| Ultimate loads from test(t) | 5.95 | 5.25 | 4.80 | 3.65 |
| Ultimate bending moment from experiment(kN-m)* | 16.78 | 14.81 | 13.54 | 10.50 |
| Ultimate bending moment from modeling(kN-m) | 15.25 | 13.76 | 13.09 | 11.82 |

*Calculation from test ultimate loads as loading in Figure 4

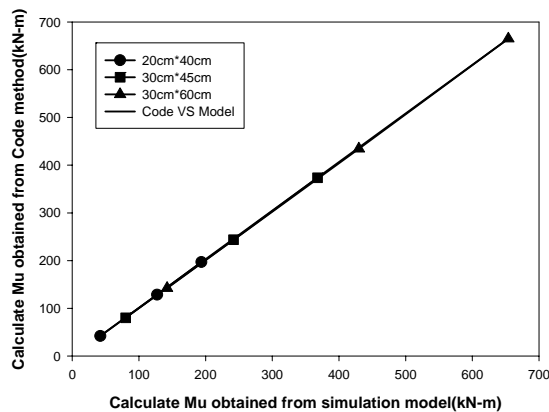


Figure 2. Comparison of ultimate bending moment (M_u) obtained from the ACI Code method and simulated results for various dimensions of beams and steel ratios

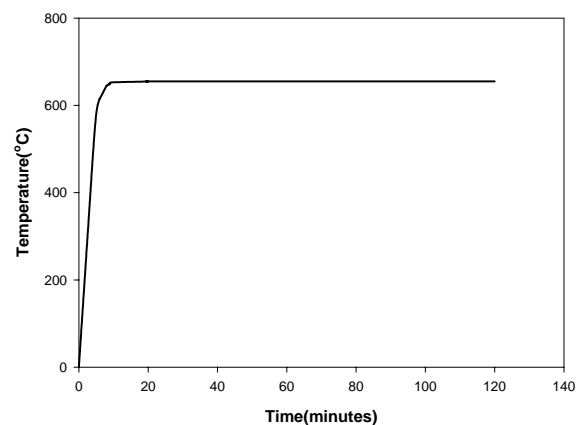
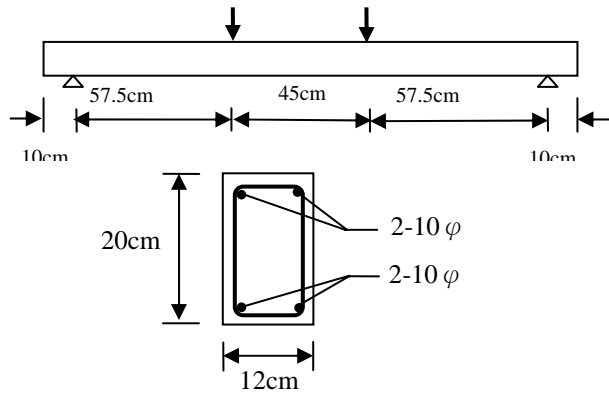


Figure 3. Time-Temperature curve



Cross-section

Figure 4. Fire flexural test conditions

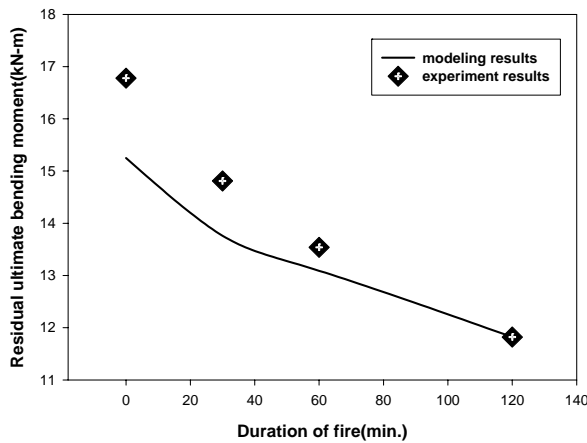


Figure 5. The decreases in residual bending moments with duration of fire

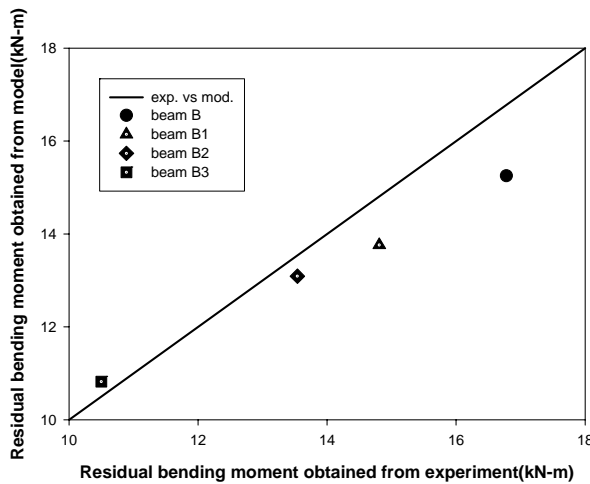


Figure 6. Comparison of residual bending moments obtained from experimental and modeling results

Lin et al. [10] fabricated 35 full-scale RC beams (Table 3) with various dimensions and parameters. All beams were cured under the same conditions in a laboratory. After curing for 28 days, the beams were placed in a gas furnace. The beams were heated according to the ASTM E 119 standard temperature-rise curve [16] through three surfaces; the beam tops were insulated. After natural cooling, the beams were loaded using the two-point method and tested to failure. Table 4 presents experimental and simulated data for residual shear force of the beams. The calculated and experimental data follow similar trends (Figure 7). The calculated values are typically less than experimental values, indicating that modeling results are conservative.

In order to realize the effects of fire on bearing capabilities of RC beams, this study simulated the residual bending moment and shear strength of RC beams heated on three surfaces (the top was insulated) with ASTM E 119 standard temperature-rise curve (Figure 8)[16]. Several Equations approximating the ASTM E 119 curve are given by Lie [17], the simplest of which gives the temperature T ($^{\circ}C$) as

$$T = 750 \left[1 - e^{-3.79553\sqrt{t_h}} \right] + 170.41\sqrt{t_h} + T_0 \quad (18)$$

where t_h is the time (hours) and T_0 is the ambient temperature ($^{\circ}C$).

The beam cross sections were rectangular at 300mm wide, 500mm deep, 4 ϕ 25 steel bars as the tensile reinforcement, 2 ϕ 25 steel bars as the tensile reinforcement and 10mm steel bar spacing of 100mm as the stirrup (Figure 9). The compressive strength of the concrete is 210kg/cm², and the yielding strength of the steel bar is 4200 kg/cm². Table 5 shows the predictions of the residual values and ratios of positive and negative bending moments with duration of fire.

The bending moment is positive when a beam tends to produce tension under neutral axis of the beam and compression above neutral axis, otherwise is negative. In continuous

structures, beams may sustained positive and negative bending moments. A beam may sustain negative bending moment in addition to positive bending moment during earthquake. While beams getting failure in negative bending moment after fire exposure means the beam may crushed by compressive failure suddenly. The effects of fire damages to the negative bending moment could be more serious than the positive bending moment. Figure 10 plots the residual ratios of positive and

negative bending moments with duration of fire. The residual ratio of positive bending moment decreased to 30.82% following exposure to fire for 240 minutes. While the beam get failure in negative bending moment when fire exposed 173 minutes. In this case, the compressive strength of concrete under neutral axial have declined because of the heated of high temperature and beam has been crushed by compressive failure suddenly.

Table 3. Full-scale RC Beams from Lin et al. [10]

| Test No. | Sample Size(cm) | Ln/d | a/d | b (cm) | d (cm) | f_c (kg/cm ²) | Tensile Steel | stirrup | Duration of Fire (hr.) |
|----------|-----------------|------|-----|--------|--------|-----------------------------|---------------|---------|------------------------|
| 1 | 20×30×160 | 4.54 | 1.5 | 20 | 26 | 347 | 3-#7 | 0 | 0 |
| 2 | 20×30×160 | 4.54 | 1.5 | 20 | 26 | 347 | 3-#7 | 0 | 1 |
| 3 | 20×30×160 | 4.54 | 1.5 | 20 | 26 | 347 | 3-#7 | 0 | 3 |
| 4 | 20×30×300 | 9.54 | 4.0 | 20 | 26 | 347 | 3-#7 | 0 | 0 |
| 5 | 20×30×300 | 9.54 | 4.0 | 20 | 26 | 347 | 3-#7 | 0 | 1 |
| 6 | 20×30×300 | 9.54 | 4.0 | 20 | 26 | 347 | 3-#7 | 0 | 3 |
| 7 | 20×30×160 | 4.67 | 1.5 | 20 | 24 | 358 | 6-#7 | 0 | 0 |
| 8 | 20×30×160 | 4.67 | 1.5 | 20 | 24 | 358 | 6-#7 | 0 | 1 |
| 9 | 20×30×160 | 4.67 | 1.5 | 20 | 24 | 358 | 6-#7 | 0 | 3 |
| 10 | 20×30×300 | 9.67 | 4.0 | 20 | 24 | 358 | 6-#7 | 0 | 0 |
| 11 | 20×30×300 | 9.67 | 4.0 | 20 | 24 | 358 | 6-#7 | 0 | 1 |
| 12 | 20×30×300 | 9.67 | 4.0 | 20 | 24 | 358 | 6-#7 | 0 | 3 |
| 13 | 20×30×160 | 4.54 | 1.5 | 20 | 26 | 347 | 3-#7 | #3@8cm | 0 |
| 14 | 20×30×160 | 4.54 | 1.5 | 20 | 26 | 347 | 3-#7 | #3@8cm | 1 |
| 15 | 20×30×160 | 4.54 | 1.5 | 20 | 26 | 347 | 3-#7 | #3@8cm | 3 |
| 16 | 30×45×200 | 4.11 | 1.5 | 30 | 36 | 347 | 6-#7 | 0 | 0 |
| 17 | 30×45×200 | 4.11 | 1.5 | 30 | 36 | 347 | 6-#7 | 0 | 1 |
| 18 | 30×45×200 | 4.11 | 1.5 | 30 | 36 | 347 | 6-#7 | 0 | 3 |
| 19 | 30×45×270 | 9.11 | 4.0 | 30 | 36 | 358 | 8-#9 | 0 | 0 |
| 20 | 30×45×270 | 9.11 | 4.0 | 30 | 36 | 358 | 8-#9 | 0 | 1 |
| 21 | 30×45×270 | 9.11 | 4.0 | 30 | 36 | 358 | 8-#9 | 0 | 3 |
| 22 | 30×45×200 | 4.11 | 1.5 | 30 | 36 | 347 | 6-#7 | #3@8cm | 0 |
| 23 | 30×45×200 | 4.11 | 1.5 | 30 | 36 | 347 | 6-#7 | #3@8cm | 3 |
| 24 | 30×45×370 | 9.11 | 4.0 | 30 | 36 | 358 | 8-#9 | #3@15cm | 0 |
| 25 | 30×45×370 | 9.11 | 4.0 | 30 | 36 | 358 | 8-#9 | #3@15cm | 3 |
| 26 | 20×30×160 | 4.54 | 1.5 | 20 | 26 | 598 | 3-#7 | 0 | 0 |
| 27 | 20×30×160 | 4.54 | 1.5 | 20 | 26 | 605 | 3-#7 | 0 | 1 |
| 28 | 20×30×160 | 4.54 | 1.5 | 20 | 26 | 625 | 3-#7 | 0 | 3 |
| 29 | 20×30×300 | 9.54 | 4.0 | 20 | 26 | 601 | 3-#7 | 0 | 0 |
| 30 | 20×30×300 | 9.54 | 4.0 | 20 | 26 | 716 | 3-#7 | 0 | 1 |
| 31 | 20×30×160 | 4.67 | 1.5 | 20 | 24 | 634 | 6-#7 | 0 | 0 |
| 32 | 20×30×160 | 4.67 | 1.5 | 20 | 24 | 652 | 6-#7 | 0 | 1 |
| 33 | 20×30×160 | 4.67 | 1.5 | 20 | 24 | 665 | 6-#7 | 0 | 3 |
| 34 | 20×30×300 | 9.67 | 4.0 | 20 | 24 | 609 | 6-#7 | 0 | 0 |
| 35 | 20×30×300 | 9.67 | 4.0 | 20 | 24 | 657 | 6-#7 | 0 | 1 |

Table 4. Comparisons of experimental data with simulated data on residual shear strength

| Test No. | Experimental data (kN) | Simulated data (kN) | Test No. | Experimental data (kN) | Simulated data (kN) |
|----------|------------------------|---------------------|----------|------------------------|---------------------|
| 1 | 177.56 | 132.53 | 19 | 138.81 | 122.57 |
| 2 | 213.86 | 104.77 | 20 | 211.90 | 104.95 |
| 3 | 188.84 | 79.66 | 21 | 117.23 | 89.17 |
| 4 | 63.57 | 52.48 | 22 | 471.66 | 389.33 |
| 5 | 48.76 | 43.75 | 23 | 467.64 | 310.08 |
| 6 | 57.68 | 27.27 | 24 | 375.04 | 250.87 |
| 7 | 276.15 | 177.36 | 25 | 311.86 | 217.48 |
| 8 | 320.98 | 149.11 | 26 | 283.71 | 161.28 |
| 9 | 220.72 | 123.61 | 27 | 337.46 | 124.36 |
| 10 | 79.85 | 54.57 | 28 | 229.46 | 92.01 |
| 11 | 89.17 | 48.33 | 29 | 89.27 | 67.54 |
| 12 | 41.30 | 32.65 | 30 | 89.76 | 59.18 |
| 13 | 289.89 | 212.35 | 31 | 466.96 | 207.30 |
| 14 | 270.56 | 184.56 | 32 | 471.37 | 170.89 |
| 15 | 243.09 | 159.45 | 33 | 246.53 | 136.98 |
| 16 | 431.84 | 287.33 | 34 | 123.21 | 68.13 |
| 17 | 468.33 | 244.39 | 35 | 130.28 | 61.91 |
| 18 | 279.00 | 208.09 | | | |

Table 5. Modeling predictions of the residual values and ratios of bending moment with duration of fire

| Duration of fire | Positive bending moment | | Negative bending moment | |
|------------------|-------------------------|-----------|-------------------------|-----------|
| | Value (kN-m) | Ratio (%) | Value (kN-m) | Ratio (%) |
| 0 min. | 306.87 | 100 | 160.37 | 100 |
| 20 min. | 295.68 | 96.35 | 147.14 | 91.76 |
| 40 min. | 286.96 | 93.51 | 140.41 | 87.56 |
| 60 min. | 271.71 | 88.54 | 134.94 | 84.14 |
| 80 min. | 245.87 | 80.12 | 130.44 | 81.34 |
| 100 min. | 221.01 | 72.02 | 125.43 | 78.21 |
| 120 min. | 199.88 | 65.13 | 119.73 | 74.66 |
| 140 min. | 181.22 | 59.05 | 112.51 | 70.16 |
| 160 min. | 162.12 | 52.83 | 103.73 | 64.68 |
| 180 min. | 143.39 | 46.73 | N* | N |
| 200 min. | 125.18 | 40.79 | N | N |
| 220 min. | 108.62 | 35.39 | N | N |
| 240 min. | 94.58 | 30.82 | N | N |

* N means the beam has been failed

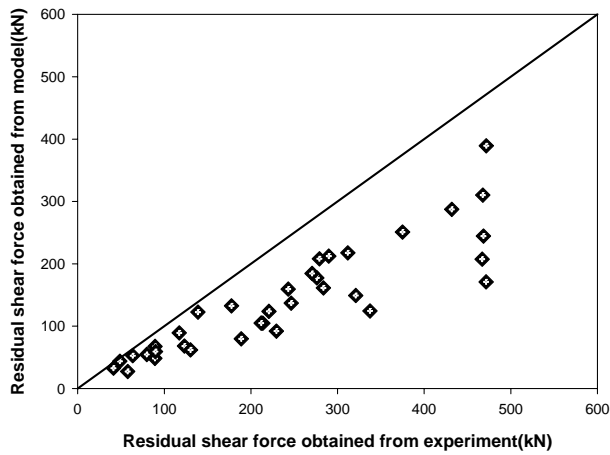


Figure 7. Comparison of residual shear forces obtained from experimental and modeling results

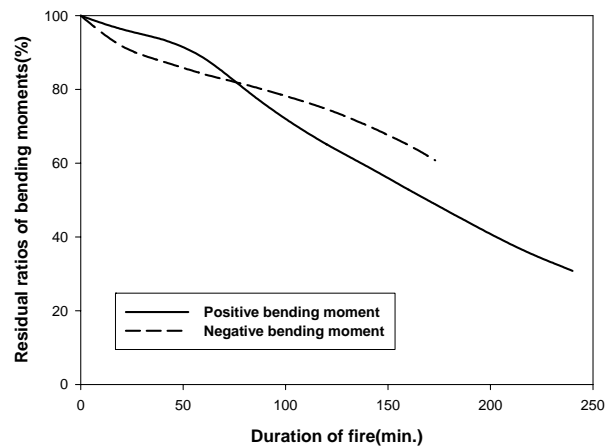


Figure 10. Residual ratios of positive and negative bending moments with duration exposed to fire

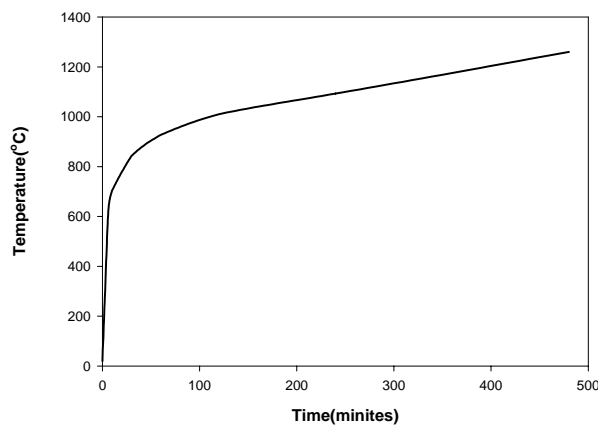


Figure 8. ASTM E119 Time-Temperature curve

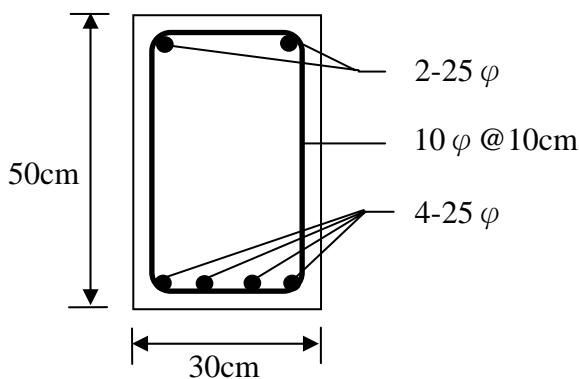


Figure 9. Cross-section of the simulated beam

The residual shear strengths and ratios provided by concrete and shear reinforcement have predicted in this model, the results are shown in Table 6. Figure 11 plots the residual of shear strength with duration of fire. The shear strength provided by concrete decreased smoothly from 102.85 kN (when first heated) to 66.60 kN (after fire exposure of 240 minutes). The residual shear strength provided by shear reinforcement remained nearly the same in the first 40 minutes of fire, but decreased quickly when started to decline. The modeling results revealed that the shear reinforcement provided the main shear strength in common states but decreased quickly when yielding strength has influenced by high temperature. The covered concrete could delay the influence of high temperature on shear reinforcement. Increasing the thickness of covered concrete is helpful to protect the damage of fire on shear strength.

5. Conclusion

This study presented a novel model for predicting residual capabilities of RC beams that are exposed to fire. The basic approach utilized by the model was validated using results

obtained by previous experiments in which full-scale reinforced concrete beams were exposed to fire. The agreement between the model and experimental data is very good. The following conclusions are drawn.

1. This study combines thermal and structural analyses for characterizing the residual bearing capabilities as well as flexural and shear capacities of reinforced concrete beams after fire exposure. As no two fires are the same, the modeling results provide valuable insights for the fire resistance and deformation characteristics of fire-damaged RC beams.
2. In continuous structures, beams may sustained positive and negative bending moments. A beam may sustain negative bending moment in addition to positive bending moment during an earthquake. RC beams that have been exposed to fire in the past, if experiencing negative bending moment, might be unexpectedly crushed by compressive failure once a critical level is surpassed. Relatively speaking, one that experiences positive bending moment will only cause the reduction of beam strength. Hence the safety of fire-damaged RC structures that sustain negative bending moment must be carefully assessed with extra attention.
3. The shear reinforcement provides the main shear strength in common states but decreases quickly when yielding strength has been influenced by high temperature. The covered concrete may delay the effect of high temperature on the strength of shear reinforcement. Increasing the thickness of covered concrete is helpful to protect the damage of fire on the shear strength.
4. The calculation in the presented model assumes that the beam section remains complete (no crack) after exposed to fire. When cracks are observed in the beam section after fire damage, the legitimacy of using this model should be further evaluated.

Appendix: list of symbols

| | |
|--------------|---|
| A_s | =area of reinforcing steel |
| A_v | =area of shear reinforcement |
| b | =width of the beam |
| C | =compressive force acting on the beam cross section |
| d | =effective depth of the beam |
| f'_c | =specified compressive strength of concrete |
| $f_{c,ij}^T$ | =concrete residual compressive stress of lump unit ij after sustaining temperature T and at strain of $\varepsilon_{c,ij}$ ($\varepsilon_{c,ij}$ denotes the strain at the center of each lump unit ij) |
| f_y | =specified yield strength of reinforcement steel |
| f_{yr} | =residual yielding strength of reinforcement steel after sustaining temperature T |
| l_n | =clear span measured face-to-face of support |
| M | =unitary numbers in beam width |
| M_u | =factored moment forced at section |
| N | =unitary numbers in beam depth |
| s | =spacing of shear reinforcement in direction parallel to longitudinal rein- |

| | |
|----------------------|--|
| | forcement |
| T | =the highest temperature that the materials have endured |
| T_{en} | = tensile force acting on the beam cross section |
| t | =time variable |
| V_c | =nominal shear strength provided by concrete |
| V_s | =nominal shear strength provided by shear reinforcement |
| V_u | =factored shear force at section |
| ρ | =ratio of reinforcement |
| $\Delta x, \Delta y$ | =width and depth of lump unit |

Reference

- [1] Gruz, C. R. 1966. Elastic Properties of Concrete at High Temperature. *Journal of the PCA Research and Development Laboratories*, 8, 1: 37-45.
- [2] Smith, E. E., and Harmathy, T.Z. 1979. "Design of Building for Fire Safety", American Society for Testing and Materials, Philadelphia.
- [3] Carman, A. D. and Nelson, R. A. 1921. "The thermal conductivity and diffusivity of concrete". Bulletin No. 122: 32, Engineering Experimental Station, University of Illinois, Urbana.
- [4] Uddin, T. and Culver, C. G. 1975. Effect of Elevated Temperature on Structure Members *Journal of structural Div. ASCE*, 101: 1531-1549.
- [5] ACI Committee 216. 1981. Guide for determining the fire endurance of concrete elements. ACI 216-81. *Concrete International*, 3: 13-47.
- [6] Kong, F. K., Evans, R. H., Cohen, E., and Rall, F. 1983. "Handbook of Structural Concrete", McGraw-Hill, New York.
- [7] Hsu, J. H., Lin, C. S., and Hung, C. B. 2006. Modeling the Effective Elastic Modulus of RC Beams Exposed to Fire. *Journal of Marine Science and Technology*, 14, 2 :1-7.
- [8] Lin, T. D. 1985. Measured Temperature in Concrete Beams Exposed to ASTM E 119 Standard Fire. "Research and Development Report", Portland Cement Association, Skokie.
- [9] Moetaz, M. E., Ahmed, M. R., and Shadia, E. 1996. Effect of Fire on Flexural Behavior of RC Beams. *Construction and Building Materials*, 10, 2: 147-150.
- [10] Lin, I. J., Chen, S. T., and Lin, C. J. 1999. The Shear Strength of Reinforcing Concrete Beam after Fire Damage. "Structure Safety Evaluation after Fire Damage", Scientific & Technical Publishing Co., Ltd., Taiwan, 117-136.
- [11] ACI 318R-02. 2002. "Building Code Requirements for Structural Concrete and Commentary", American Concrete Institute, Michigan.
- [12] Buchanan, A. H. 2000. "Structure Design for Fire Safety". JOHN WILEY & SONS, LTD.
- [13] Çengel, Y. H. 1998. "Heat Transfer: a practical approach", (International Edition), McGraw-Hill, 57-111
- [14] Eurocode 3. Design of Steel Structures. ENV 1993-1-2, 1995. General Rules – Structural Fire Design. "European Committee for Standardization", Brussels, Belgium.
- [15] Abrams, M. S. 1968. Compressive Strength of Concrete at Temperature to 1600 °F. "Temperature and Concrete", ACI Publication SP25, 33-58.
- [16] ASTM E05.11 Task Group. 1982. "Repeatability and reproducibility of Results of ASTM E 119 Fire Test", Research Report No. RR: E5-1003, ASTM, Philadelphia.

- [17] Lie, T. T. 1995. Fire Temperature-Time Relations. “*SFPE Handbook of Fire Protection Engineering*”, Second Edition. Society of Fire Protection Engineers, USA.

